JOURNAL OF MATERIALS SCIENCE 28 (1993) 5461–5468

Electrocal, thermal, thermoelectric and related properties of magnesium silicide semiconductor prepared from rice husk

S. BOSE‡, H. N. ACHARYA
Energy Research Unit, Indian Association for the Cultivation of Science (IACS), Jadavpur, Calcutta 700032, India

H. D. BANERJEE
Materials Science Centre and Department of Physics, Indian Institute of Technology, Kharagpur 721 302, India

Polycrystalline, 10 μm size magnesium silicide was prepared by alloying 99.9% purity polycrystalline silicon obtained from rice husk ash and high-purity magnesium powder. The material in sintered pellet form was characterized for its structural, electrical, thermal, thermoelectric and other properties. A typical sintered pellet exhibited a room-temperature (30 °C) thermoelectric power of 565 $\mu V K^{-1}$ and an electrical resistivity of 35 Ω cm. On the other hand, the material was found to be thermally quite stable up to 650 °C with a room-temperature thermal conductivity of 6.3×10^{-3} cal $s^{-1} cm^{-1} K^{-1}$ (2.6 J $s^{-1} m^{-1} K^{-1}$). These properties of the material indicate that the material can find potential applications as a thermoelectric generator and in other semiconductor devices. Furthermore, an indigenous technology for large-scale production of silanes (SiH_4) can be developed using this Mg_2Si which could be prepared in large quantities by a simple and low-cost process.

1. Introduction

Magnesium silicide (Mg_2Si) is a semiconductor having antifluorite crystal structure in which the silicon atoms forms an fcc lattice with lattice constant $a = 0.6391$ nm. This compound has an optical band gap of 0.76 eV and reasonably high mobility of 350 $cm^2 V^{-1} s^{-1}$ (for electrons) [1]. It can be doped with both n- and p-type impurities with large thermoelectric power and low thermal conductivity $k = 6.3 \times 10^{-3}$ cal s^{-1} cm^{-1} K^{-1} [2]. These properties of the material indicate that the material may find potential applications as photoconducting, photovoltaic and thermoelectric device materials. All undoped crystals of Mg_2Si are n-type; however, p-type materials can also be prepared by doping with silver and copper with saturation carrier concentrations of 7×10^{17} and 4×10^{17} cm^{-3}, respectively [1–3]. On the basis of studies on the electrical conductivity and Hall effect (77–1000 K), the authors reported that the Hall mobility was temperature-dependent in the intrinsic range ($\simeq T^{-5/2}$) and at 300 K its value was as high as 406 $cm^2 V^{-1} s^{-1}$ for n-type and 56 $cm^2 V^{-1} s^{-1}$ for p-type materials. The electron to hole mobility ratio and energy gap as determined in their studies were 5 and 0.78 eV, respectively.

The crystals of Mg_2Si were grown by the Bridgman technique wherein relatively large and homogeneous samples were obtained [1–6]. Thermal conductivities of such crystals were measured by Lobotz and Mason [2] using a dynamic calorimeter from 0 to 300 °C. The contribution due to phonon scattering to the thermal conductivity was reported to be more predominant than the electronic contribution in this material. The thermal conductivity of n-type Mg_2Si was also measured from liquid nitrogen temperature to 30 °C by Martin [6]. Stella and Lynch [4] in their studies on the photoconducting properties of this material observed that the surface recombination of carriers was rapid in Bridgman-grown n-type specimens, with a bulk lifetime of about 10^{-4} s. The photoresponse curve exhibited a peak at 0.69 eV. Reflectance measurements from 0.6 to 11 eV at 77 K were carried out by Scowler [3], who reported that although Mg_2Si crystallized in antifluorite structures, their optical properties were similar to those of zinc-blende structure semiconductors. The Seebeck coefficients, resistivities and Hall coefficients of single crystals of material grown by the Bridgman technique were measured between 77 and 100 K by Heller and Danielson [5].

Looking at the properties of this material and from the facts and figures stated above, it can be concluded that Mg_2Si is not only a useful semiconductor material which may find many important device applications; it is, in particular, a potential candidate material for efficient thermoelectric generator devices (high value of figure of merit $Z = \alpha^2\sigma/k$, where α is the thermoelectric power, σ is the electrical conductivity and k is the thermal conductivity). On the other hand, it is well known that Mg_2Si is the only basic raw

material used for preparing silanes and disilanes needed for the manufacture of semiconductor-grade amorphous and crystalline silicon. The present manufacturing process of Mg_2Si involves the alloying of commercially available high-purity and costly polysilicon and magnesium metal, resulting in a high cost of production of this material.

In view of the above, a comprehensive programme has been undertaken in our laboratory to develop a simple, high-volume and low-cost technique for preparing high-purity polysilicon and magnesium silicide from rice husk ash. A substantial amount of work on preparing high-purity polysilicon from rice husk ash has already been done and some important and interesting results of those investigations were published. Reasonably pure (99.9 %, 10 μm size) polysilicon was prepared from rice husk ash and its detailed characterization was undertaken [7–10]. Using this rice husk polysilicon and high-purity magnesium, Mg_2Si was prepared in large quantities by the alloying technique. The material was then characterized in detail by studying its structural, electrical, thermal, thermoelectric and other related properties. The results of these investigations and some essential conclusions are reported in this paper.

2. Experimental procedure

2.1. Material preparation

About 20 kg of rice husks were collected from a nearby rice milling plant. They were washed with water to remove dirt and other contaminants present in them and then sun-dried. The cleaned husks were then burnt inside a muffle furnace under controlled conditions of air flow, the details of which were reported in our earlier work [7]. The ash obtained after the complete burning of husks was leached with conc. HCl (11.3 N) for 2–3 h under boiling conditions to remove soluble inorganic impurities present in them. The acid-leached mass was then thoroughly washed with deionized water to make them completely acid-free, and subsequently filtered. The material was then dried in an air oven at about 60 °C. Thus a 99.9 % pure, milky-white fine powder of amorphous silica (SiO_2), called "white ash", was obtained.

Appropriate amounts of prepared white ash and commercially available 99.9 % pure magnesium powder were thoroughly mixed and then tightly packed in an MgO-coated (inside) selemenite crucible and then fired at about 650 °C inside a muffle furnace. The amorphous SiO_2 was thus reduced to form silicon according to the following reaction:

$$SiO_2 + 2Mg = Si + 2MgO + SiO_2 \text{ (unreacted)}$$

The resulting mass after reduction was successively leached with conc. HCl and HF to remove MgO and unreacted SiO_2, respectively, from the reaction product. The acid-leached material was then thoroughly washed with deionized water, filtered and dried. Details of the preparation technique were given in our earlier communication [7]. Reasonably pure (99.9 %), 10 μm size polysilicon was thus obtained and then used for preparing Mg_2Si by the alloying technique.

Appropriate quantities of rice husk silicon and magnesium powder (both 99.9 % pure) were intimately mixed and then fired inside an alloying furnace at 500 °C for 24 h under an H_2 atmosphere (high purity, IOLAR-II H_2). The alloying took place according to the reaction

$$Si + 2Mg = Mg_2Si$$

The temperature of the alloying furnace was controlled within ± 2 °C. After completion of the reaction, a deep blue powdery Mg_2Si material was obtained. In this way about 100 g of the material was prepared and then immediately stored inside a vacuum desiccator. Some of this material was then pelletized by applying a pressure of 5 tonne cm^{-2} in a hydraulic press. A good number of such pellets were prepared and then they were sintered inside a sintering furnace under an argon (IOLAR-II) atmosphere at 550 °C for 24 h.

2.2. Characterization

2.2.1. X-ray diffraction and other structural property studies

X-ray diffraction (XRD) studies on the material were undertaken using a Philips X-ray diffraction unit (model PW 1710, MoK_α radiation). The X-ray diffractogram was analysed and the d values corresponding to Mg_2Si were identified. The grain size of the material was calculated by using the Scherrer formula.

2.2.2. SEM studies and energy-dispersive X-ray analysis (EDAX)

Scanning electron microscopic examination of the pellet was conducted using an SEM–Camscan series 2 unit at appropriate magnification. The sizes of the grains were measured from the micrographs. This particular pellet was then used for all other studies. The SEM studies were conducted in the secondary electron mode to give details of the surface morphology.

2.2.3. Electrical conductivity studies

The electrical conductivities of the sintered pellets were measured at different temperatures by adopting a two-point probe technique inside a specially designed tubular furnace in an argon atmosphere. Silver paint contacts were found to give ohmic behaviour.

2.2.4. Thermoelectric power measurement

Thermoelectric power measurements on the pellets were conducted using a specially designed experimental set-up fabricated in our laboratory (Fig. 1). The sample was held in a position in a U-shaped metallic clamp with two studs, one of which was fixed while the other could be moved. The thermoelectric power at a desired mean temperature was measured by creating a temperature difference (10 °C) between

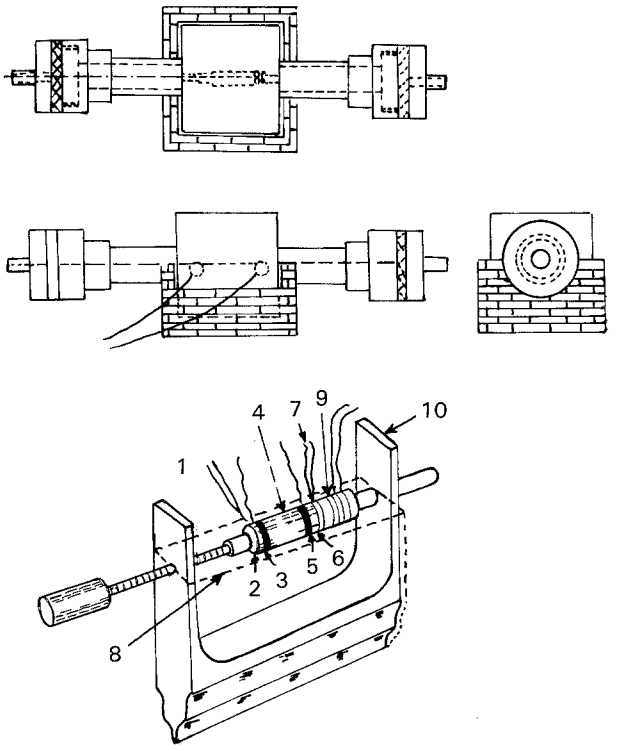

Figure 1 Schematic diagram of experimental set-up for studying electrical conductivity and thermoelectric power of sintered Mg_2Si pellets: (1, 7) thermocouples, (2, 6) alumina plates, (3, 5) nickel contacts, (4) sample, (8) copper cover, (9) heater, (10) stainless steel frame.

the two ends of the sample, using an auxiliary heater. The end temperatures of the samples were determined using copper–constantan thermocouples in conjunction with digital microvoltmeters. The temperature of the main furnace used for study of the thermoelectric power at different temperatures was maintained constant within $\pm 2\,^{\circ}C$ with the help of a temperature controller.

2.2.5. Thermal conductivity studies

Thermal conductivities of the samples were measured in an argon atmosphere using an experimental set-up designed and fabricated in our laboratory. The set-up consisted essentially of a heater assembly (heat source), a specially designed chamber and a heat sink. The sample was held between two copper rods. One of them (upper) was heated using a heater fixed above and alongside it. The above assembly of copper rod and the heater was fixed in a brass chamber which was thermally insulated by putting graphite felt inside it. The other copper rod (lower) which held the sample and whose position could be adjusted to accommodate various sample dimensions was inserted in a massive copper block which acted as a heat sink.

2.2.6. Differential thermal analysis (DTA) and thermogravimetric analysis (TGA)

One of the typical (largest grain size) specimens was subjected to DTA and TGA using a Stanton–Redcraft (STA-780 series) thermal analyser. The analysis was conducted in the temperature range 30–650 °C in argon with a uniform rate of heating ($10\,^{\circ}C\,min^{-1}$). Calcined alumina powder was used as the thermally inert reference material.

3. Results and discussion

When magnesium silicide was prepared as described above, the X-ray diffractogram revealed that the material was polycrystalline. The X-ray diffraction data are presented in Table I. From these data it was clear that the alloying reaction was complete and polycrystalline Mg_2Si was produced. The interplaner spacings and $(h\,k\,l)$ values compared well with the standard diffraction data. The average particle size of the material was calculated using the Scherrer formula and found to be 0.035 μm. The material was then thoroughly ground in a pestle and mortar and sieved to various mesh sizes. X-ray diffraction studies on each grain-size material were conducted, and from diffraction data using the Scherrer equation the grain sizes of all the materials were calculated. The values were found to be 0.086, 0.072, 0.064 and 0.050 μm for $(-85+100)$ BSS, $(-100+120)$ BSS, $(-120+150)$ BSS and $(-150+200)$ BSS sieve sizes, respectively.

Various grain-size materials thus obtained were pelletized by applying a pressure of 5 ton in^{-2} for 60 s at 30 °C. These pellets were finally sintered in an argon atmosphere for 24 h. The densities of the pellets were determined and the values are presented in Table II. It is seen from the table that lower grain-size pellets were more dense. This may be attributed to the compaction being greater for smaller grain sizes. One typical

TABLE I X-ray diffraction data of the material

Interplaner spacing (nm)	Indices of reflecting planes[a]
0.369	1 1 1
0.320	2 0 0
0.226	2 2 0
0.193	3 1 1
0.184	2 2 2
0.160	4 0 0
0.147	3 3 1
0.143	4 2 0
0.130	4 2 2
0.123	5 1 1
0.113	4 4 0
0.108	5 3 1
0.101	6 2 0
0.085	6 4 2

[a] All Mg_2Si.

TABLE II Density of magnesium silicide for mesh sizes prepared by alloying technique

BSS mesh sizes	Density ($g\,cm^{-3}$)
$-85+100$	1.84
$-100+120$	1.87
$-120+150$	1.90
$-150+200$	1.94

densely packed pellet was then examined by SEM and simultaneous EDAX analysis. Fig. 2 shows SEM of the specimen. The micrograph clearly reveals a regular distribution of particles of Mg_2Si, densely packed with very few voids. Fig. 3 shows the EDAX spectra from a location in the pellet, indicating the material to be stoichiometric Mg_2Si with no impurities in it within the detection limit of the instrument (0.5 %).

From studies on the electrical conductivity of a particular specimen (0.086 μm size) it was observed that at 30 °C the resistivity of the material was 35 Ω cm. The variation of electrical conductivity with temperature (ln σ versus $1/T$) for different grain-size pellets was studied in an argon atmosphere and the results are shown in Fig. 4. The electrical conductivity was found to be smaller for smaller grain-size materials. The activation energy for each curve was calculated and found to vary from 0.112 to 0.067 eV as the grain size of the material varied from 0.086 to 0.050 μm.

The variation of thermoelectric power (α) with temperature (T) was studied for all grain-size material pellets in an argon atmosphere, and the results are shown in Fig. 5. The room-temperature thermoelectric power (TEP) of the specimen which showed a resistivity of 35 Ω cm was found to be 565 μV K^{-1}. It may be pointed out here that this value of TEP is quite high and compares well with the TEP values ($\simeq$700 μV K^{-1}) of commercially available Si–Ge alloy or Bi_2Te thermoelectric generator materials in Bridgman-grown crystal form.

The results indicate that the materials were non-degenerate semiconductors. The thermoelectric power curves passed through a maximum at around 400 °K and TEP values were greater for larger grain-size material, decreasing continuously with decreasing grain size. The variation of activation

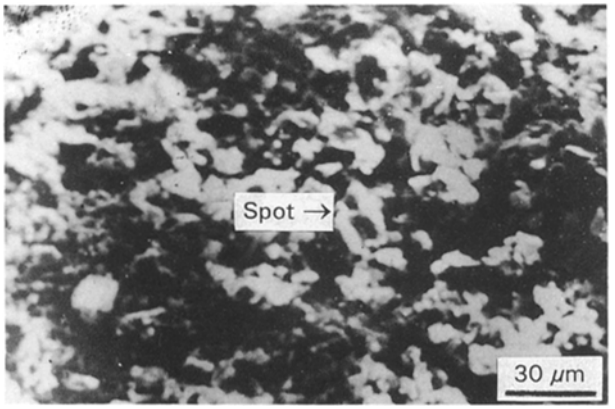

Figure 2 Scanning electron micrograph of a typical pellet of Mg_2Si.

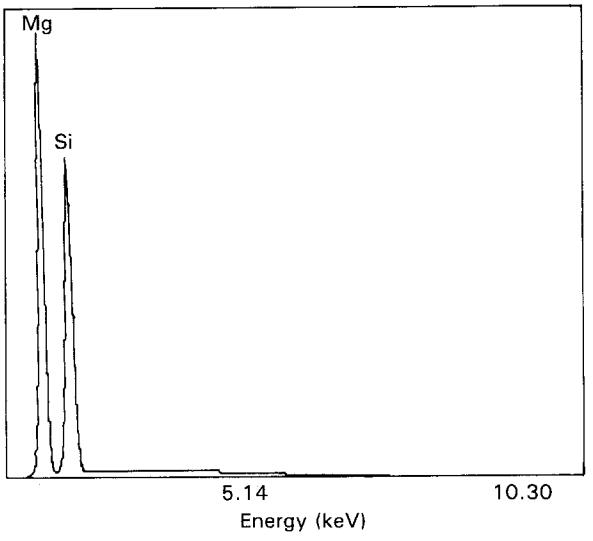

Figure 3 Energy-dispersive X-ray spectra of a representative location in the pellet of Mg_2Si.

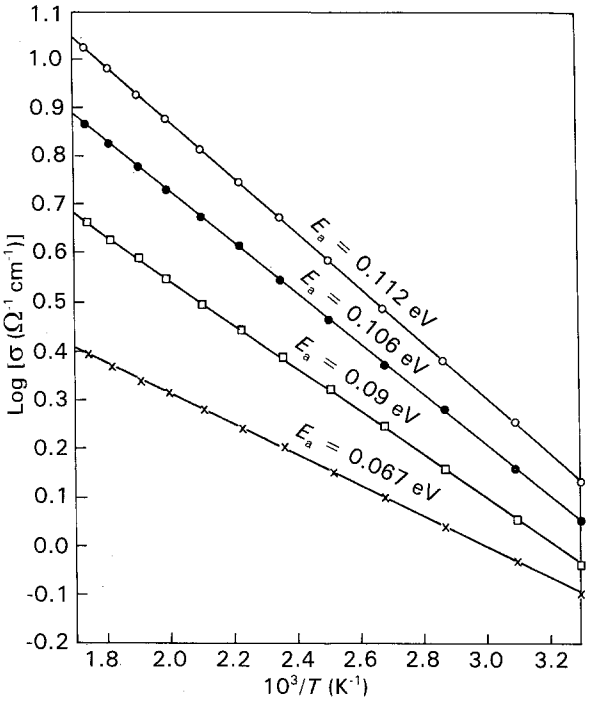

Figure 4 log σ versus $1/T$ plots obtained from variation of electrical conductivity with temperature studies on Mg_2Si pellets of various particle-size materials: (○) (− 85 + 100) BSS, (●) (− 100 + 120) BSS, (□) (− 120 + 150) BSS, (×) (− 150 + 200) BSS.

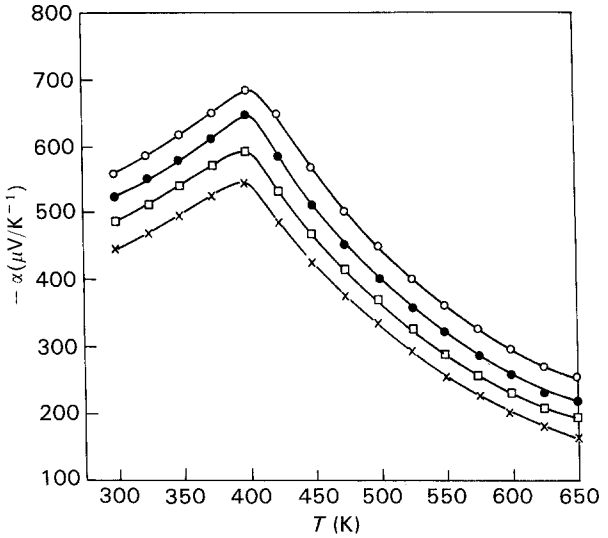

Figure 5 Variation of thermoelectric power α with absolute temperature T for pellets of various grain-size materials: (○) (− 85 + 100) BSS, (●) (− 100 + 120) BSS, (□) (− 120 + 150) BSS, (×) (− 150 + 200) BSS.

energy with particle size of the material can be understood by considering the X-ray diffraction data and SEM results (Fig. 2). These studies revealed that Mg_2Si was essentially polycrystalline. Amongst the different models correlating the transport properties in polycrystalline semiconductors proposed so far [11–18], the one proposed by Petritz [15] is perhaps the most cited theoretical analysis of transport mechanisms in polycrystalline semiconductors. The model is based upon a material in which the thermionic emission of carriers is prevalent. Our results on electrical conductivity and thermoelectric power can be very well explained by this model. Considering a single grain and a single boundary or barrier, the total resistivity of the specimen can be expressed as

$$\rho_g = \rho_1 + \rho_2 \tag{1}$$

where the subscripts signify grain or crystallite (1) and boundary (2) regions, respectively. Assuming $\rho_2 \gg \rho_1$, the expression for the current density obtained by Petritz was

$$j = \left[q\mu_0 n \exp\left(\frac{-q\phi_b}{kT}\right)\right]\xi \tag{2}$$

where $\mu_0 = M/n_c kT$, ξ is the electric field, ϕ_b is the potential height of the barriers, M is a factor which is barrier-dependent but independent of ϕ_b, n is the carrier concentration and n_c is the number of crystallites or grains per unit length.

Now since

$$j = \sigma\xi \tag{3}$$

equating Equations 2 and 3, the expression for conductivity is

$$\sigma = \frac{qMn}{n_c kT}\exp\left(-\frac{q\phi_b}{kT}\right) \tag{4}$$

Since $q\phi_b = E_b$ (the energy at the barrier) we have

$$\sigma = \frac{qMn}{n_c kT}\exp\left(-\frac{E_b}{kT}\right) \tag{5}$$

From this relation it is clear that the electrical conductivity will vary inversely with the number of crystallites per unit length. On the basis of this, our results of higher conductivity for larger grain size of the material can be explained. The energy at the barrier, E_b, can be calculated from

$$E_b = \frac{q^2 l^2 n}{8\varepsilon} \tag{6}$$

(given by Seto [19]) where l is the grain size, ε the dielectric constant (= 20 for Mg_2Si) and n the carrier concentration, which for a non-degenerate semiconductor is given by

$$\alpha = \frac{k}{q}\left[A + \ln\left(\frac{N_c}{n}\right)\right] \tag{7}$$

where α is the thermoelectric power and A is a constant whose value for n-type Mg_2Si is 1.4 [5]. Substituting these values in Equation 6, the values obtained for E_b in our studies are $E_b = 0.25$ eV for (−85 + 100) BSS and $E_b = 0.08$ eV for (−150 + 200) BSS. This explains clearly the increase of activation energy with increase in grain size of the material.

The values of activation energy obtained in our studies did not coincide with the theoretically calculated values, possibly because the grains were not identical as assumed in the theory. It may be mentioned that such grain-size variation was also revealed in SEM of the material (Fig. 2). Seto [19] proposed two conditions for correlation of conductivity with activation energy. Firstly, if Q_t is the trap density (assumed to be 10^{12} cm^{-1}), then the product $ln < Q_t$ when the grain is completely depleted of carriers and the traps are partially filled. In such a case the conductivity of the grain is given by

$$\sigma = \exp\left[-\left(\frac{E_g}{2} - E_f\right)\Big/kT\right] \tag{8}$$

whereas for the other condition when $ln > Q_t$ (i.e. when only part of the crystallite is depleted of carriers) the conductivity of the grain is given by

$$\sigma = T^{-1/2}\exp\left(-\frac{E_b}{kT}\right) \tag{9}$$

Since the calculated values of ln in the present case are 1.50×10^{12} for 0.086 μm grain size and 2.58×10^{12} for 0.050 μm, it appears that the second condition (Equation 9) is valid for this case. It shows that the activation energy of conductivity will be related to E_b. Since E_b increases with grain size (Equation 6), a higher activation energy was observed for higher grain sizes.

The TEP variation with temperature is as shown in Fig. 5. The curves for each grain size pass through a maximum. This behaviour supports the results reported by Jhonston [20]. According to him, in the temperature range studied (300–600 °K) the concentration of holes is comparable to the concentration of electrons, and in that case the thermoelectric power can be expressed as

$$\alpha = \frac{1}{nb + p}\left(\frac{k}{e}\right)\left\{p\left[A_p - \ln\left(\frac{p}{\gamma T^{3/2}}\right)\right] - nb\left[A_n - \ln\left(\frac{n}{\gamma T^{3/2}}\right)\right] - (p - nb)\ln\left(\frac{h^3}{2(2\pi m_0 k)^{3/2}}\right)\right\} \tag{10}$$

where b is the mobility ratio (3.5 for Mg_2Si), γ is the ratio of Hall to drift mobility whose value at this temperature region is 1.1, $A_n = 2.0$ and $A_p = 4.2$ [5]. Substituting these values in Equation 10, a theoretical curve for the variation of TEP with temperature can be obtained (Fig. 6). Our results on the variation of TEP with temperature for Mg_2Si agree very well with Jhonston's theory. Furthermore, our results reveal that at any particular temperature of observation the TEP increased continuously with grain size. This phenomenon can be explained by considering that if α_c is the thermoelectric power of a crystallite and α_b is the value for the boundary, the Seebeck voltage developed across the crystallite will be $\alpha_c \Delta T_c$ and at

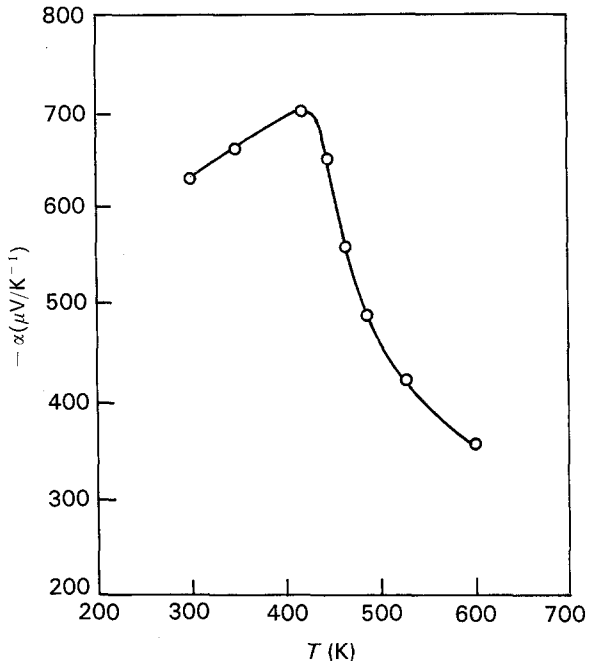

Figure 6 Variation of theoretically calculated thermoelectric power as a function of absolute temperature.

the boundary it will be $\alpha_b \Delta T_b$. Therefore α_{eff}, the total voltage developed across a unit consisting of a grain and a boundary, is given by

$$\alpha_{eff} \Delta T = \alpha_c \Delta T_c + \alpha_b \Delta T_b \quad (11)$$

where T_c and T_b are the temperature drops across the crystallite and the boundary, respectively.

If α_b is considered to be very small, then $\alpha_b \Delta T_b$ can be neglected as compared to $\alpha_c \Delta T_c$. Consequently, Equation 11 reduces to

$$\alpha_{eff} = \alpha_c \frac{\Delta T_c}{\Delta T} \quad (12)$$

Further, the total temperature drop across the unit, ΔT, is given by $\Delta T = \Delta T_c + \Delta T_b$. Again T_c across the grain is proportional to the thermal resistance offered by the grain (R_c) which can be expressed as $R_c = (1/K_c A) L_c$ where L_c is the length of the crystallite, K_c is the thermal conductivity and A is a constant. On the other hand, R_c is proportional to T_c and for larger grains T_c will be more than for smaller grains. In other words, one can write

$$(\Delta T_c)_{\text{larger grain}} > (\Delta T_c)_{\text{smaller grain}}$$

or

$$(\Delta T_c/\Delta T)_{\text{larger grain}} > (\Delta T_c/\Delta T)_{\text{smaller grain}}$$

Thus, from Equation 11 one can write

$$(\alpha_{eff})_{\text{larger grain}} > (\alpha_{eff})_{\text{smaller grain}}$$

Our results on the variation of TEP with grain size of the material at all temperatures support the above theory. The thermoelectric power of Mg_2Si was found to vary considerably with grain size in all cases and at all temperatures.

Fig. 7 shows the variation of the total thermal conductivity of the material with temperature. At room temperature (30 °C), the larger grain-size

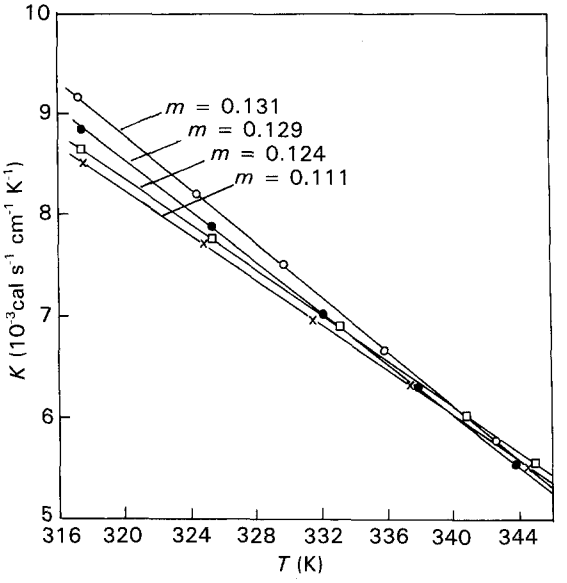

Figure 7 Variation of total thermal conductivity K with temperature (hot surface) of Mg_2Si material: (○) (− 85 + 100) BSS, (●) (− 100 + 120) BSS, (□) (− 120 + 150) BSS, (×) (− 150 + 200) BSS.

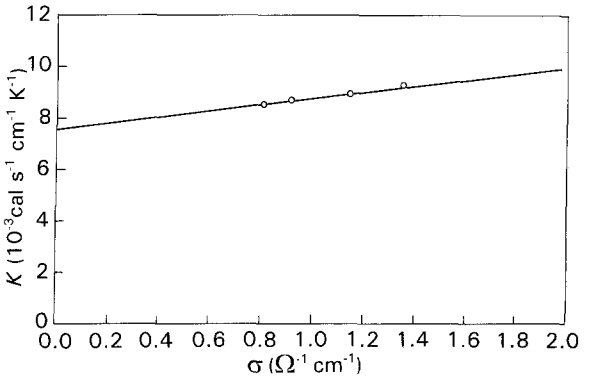

Figure 8 Total thermal conductivity of Mg_2Si as a function of its electrical conductivity. $R_L = 7.5 \times 10^{-3}$ cal s^{-1} cm^{-1} K^{-1}, $\beta = 1.18 \times 10^{-3}$ (1 cal = 4.1868 J).

material showed a thermal conductivity 9.3 $\times 10^{-3}$ cal s^{-1} cm^{-1} K^{-1} (3.9 J s^{-1} m^{-1} K^{-1}). In general, the thermal conductivity decreased with temperature and increased with the grain size. These results are in agreement with the results from many other semiconductors reported by Rowe and Bhandari [21]. Our results on the temperature variation of thermal conductivity can be explained by considering that the total thermal conductivity of the material is

$$k = k_L + k_{el} = k_L + L_0 \sigma_T \quad (13)$$

where k_L is the lattice part and k_{el} is the electronic part of the total thermal conductivity; k_{el} is related to the electrical conductivity of the material by the Weideman–Franz law [22]

$$k_{el} = L_0 \sigma_T \quad (14)$$

where L_0 is a constant known as the Lorentz number, given by the expression $L_0 = A(k/e)^2$ where A is a constant. Equation 14 can therefore be rewritten as

$$\frac{k_{el}}{\sigma} = A\left(\frac{k}{e}\right)^2 T \quad (15)$$

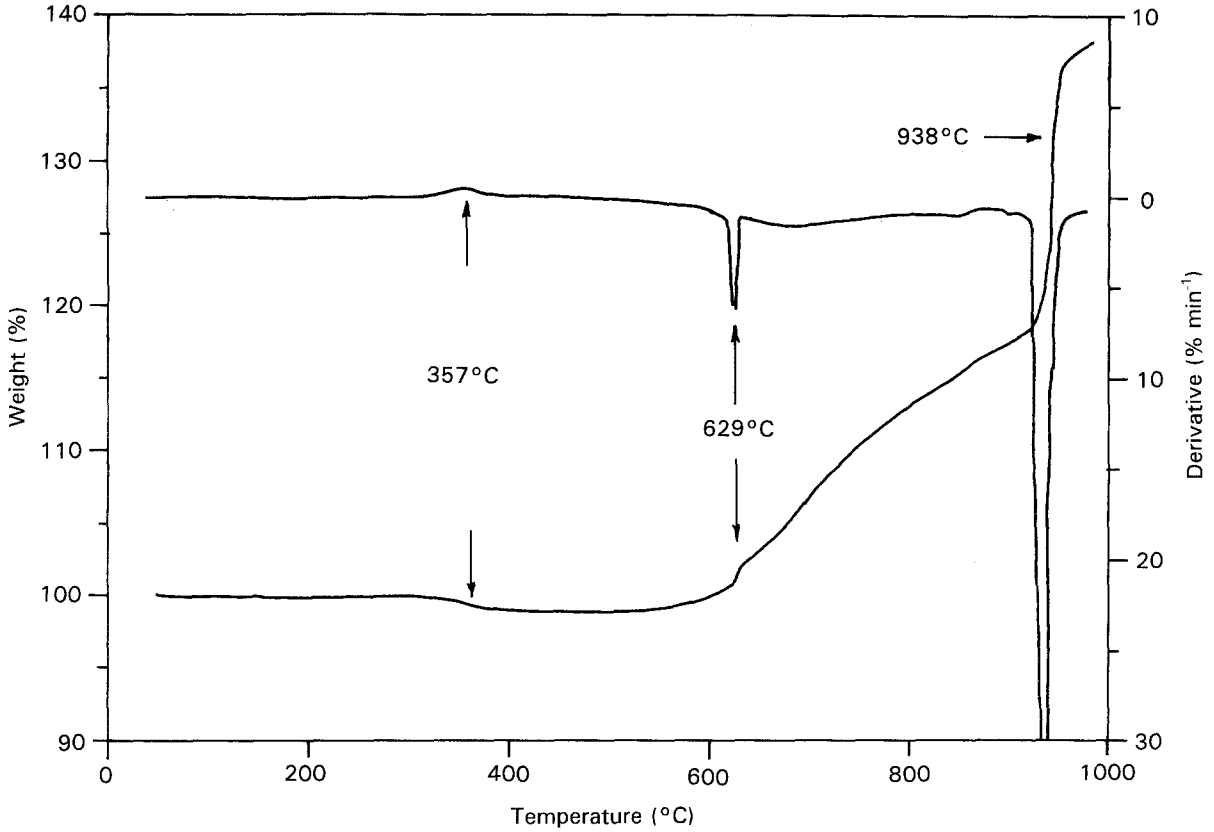

Figure 9 Differential thermal analysis and thermogravimetric analysis of (a) Mg and Si mixture, (b) sintered Mg_2Si pellet.

For a non-degenerate semiconductor, if the mean free path L is independent of the energy E of electrons, then $A = 2$. Thus the electronic part of the thermal conductivity can be separated out from the lattice part by plotting the total thermal conductivity against electrical conductivity [23, 24]. The intercept at zero electrical conductivity will give the lattice part of the thermal conductivity at that temperature. Such a plot of our results is shown in Fig. 8. The electronic part of the thermal conductivity was given by the modified Wiedman–Franz law [25], wherein it was shown that while the lattice part would vary inversely as temperature, the electronic part would be a slowly varying function of temperature. These facts clearly explain, therefore, the observed temperature and grain-size dependence of thermal conductivity of our results.

In order that a material can be effectively used for making solar energy devices, it needs to be thermally quite stable up to the temperature of operation of the device. Keeping this in mind, one of the pellets of Mg_2Si was subjected to DTA and TGA. The recorded DTA and TGA curves are shown in Fig. 9. The DTA record did not reveal any phase change or other reaction when the sample was heated from 30 to 980 °C at a uniform heating rate (10 °C min^{-1}). On the other hand, the TGA record exhibited an initial loss in weight up to about 75 °C and thereafter the weight of the material remained almost constant until 620 °C. These results clearly indicated thermal stability of the material up to 600 °C. The initial loss in weight of the material in the TGA record was possibly due to the escape of moisture contained in the specimen pellet. In order to confirm this, one specimen pellet was initially heated in a furnace in an argon atmosphere for 4 h, then cooled down to room temperature and immediately transferred to the TGA apparatus. This TGA record did not show any apparent loss in weight when heated up to 620 °C.

In addition, the TGA curves showed two weight losses at around 629 and 930 °C. These are believed to be due to sublimation of magnesium from the material around these temperatures. From the room-temperature values of α, σ and k of a typical large grain-size pellet, the figure of merit was calculated and found to be $0.910 \times 10^{-4} \simeq 1 \times 10^{-4}$, whereas the figures of merit of commercially exploited thermoelectric generator materials like Bi_2Te_3 and Si–Ge are 2.5×10^{-3} and 1.7×10^{-3}, respectively.

References

1. R. G. MORRIES, R. D. REDIN and G. C. DANIELSON, *Phys. Rev.* **109** (1958) 1909.
2. R. J. LOBOTZ and D. R. MASON, *J. Electrochem. Soc.* **110** (1963) 121.
3. W. J. SCOWLER, *Phys. Rev.* **178** (1969) 1353.
4. A. STELLA and D. W. LYNCH, *J. Phys. Chem. Solids* **25** (1964) 1253.
5. M. W. HELLER and G. C. DANIELSON, *ibid.* **23** (1962) 601.
6. J. J. MARTIN, *ibid.* **32** (1972) 1139.
7. H. N. ACHARYA, H. D. BANERJEE and S. SEN, in Proceedings of National Solar Energy Convention, Bombay, December 1979, p. 296.
8. H. N. ACHARYA, S. K. DUTTA and H. D. BANERJEE, *Solar Energy Mater.* **3** (1980) 441.
9. H. D. BANERJEE, S. SEN and H. N. ACHARYA, *Mater. Sci. Engng* **52** (1982) 173.
10. D. N. BOSE, P. A. GOVINDACHYALU and H. D. BANERJEE, *Solar Energy Mater.* **7** (1982) 319.

11. W. H. HALL, G. K. WILLIAMSON, *Proc. Phys. Soc. B* **64** (1951) 937.
12. S. CHATTERJEE, H. N. ACHARYA and V. V. RATNAM, *J. Mater. Sci.* **22** (1987) 2793.
13. L. L. KAZMERSKI (ed.), "Polycrystalline and Amorphous Thin Films and Devices", (Academic, New York, 1980) p. 87.
14. J. VOLGER, *Phys. Rev.* **9** (1950) 1023.
15. R. L. PETRITZ, *ibid.* **104** (1956) 1508.
16. H. BERGER, *Phys. Status Solidi* **1** (1961) 739.
17. R. G. MANKARIOUS, *Solid State Electron.* **7** (1964) 702.
18. Z. T. KUZNICKI, *Thin Solid Films* **33** (1976) 349.
19. J. Y. W. SETO, *J. Appl. Phys.* **46** (1975) 5247.
20. V. A. JHONSTON, in "Progress in Semiconductors", Vol. 1 (Wiley, New York, 1956) p. 65.
21. D. M. ROWE and C. M. BHANDARI, in "Modern Thermoelectrics" (Holt Reinhart and Winston, London, 1983).
22. Yu. I. RAVICH, B. A. EFIMORA and I. A. SMIRNOV, in "Semiconducting Lead Chalcogenides" (Plenum, New York, 1970).
23. J. R. DRABBLE and H. J. GOLDSMID, in "Thermal Conduction in Semiconductors" (Pergamon, New York, 1961).
24. A. F. IOFFE, in "Physics of Semiconductors" (Infosearch, London, 1960).
25. S. CHATTERJEE, PhD thesis, Indian Institute of Technology, Kharagpur (1987).

Received 28 May 1992
and accepted 16 March 1993